Wall shape optimization for a thermosyphon loop featuring corrugated pipes

EINDHOVEN UNIVERSITY OF TECHNOLOGY
Department of Mathematics and Computer Science

CASA-Report 11-44
September 2011

Wall shape optimization for a thermosyphon loop featuring corrugated pipes

by

P.I. Rosen Esquivel, J.H.M. ten Thije Boonkkamp,
J.A.M. Dam, R.M.M. Mattheij

Centre for Analysis, Scientific computing and Applications
Department of Mathematics and Computer Science
Eindhoven University of Technology
P.O. Box 513
5600 MB Eindhoven, The Netherlands
ISSN: 0926-4507

WALL SHAPE OPTIMIZATION FOR A THERMOSYPHON LOOP FEATURING CORRUGATED PIPES

P. I. Rosen Esquivel[1], Jan H.M. ten Thije Boonkkamp[1], Jacques A.M. Dam[2], Robert M.M. Mattheij[1]

[1]CASA, Dept. of Math. and Comp. Science, Eindhoven University of Technology, Eindhoven, 5600 MB, The Netherlands

[2]Imtech SMS, The Hague, 2491 AC, The Netherlands

ABSTRACT

In the present paper we address the problem of optimal wall-shape design of a single phase laminar thermosyphon loop. The model takes the buoyancy forces into account via the Boussinesq approximation. We focus our study on showing the effects of wall shape on the flow and on the temperature inside the thermosyphon. To this extend we determine the dependency of the flow rate and the increase in temperature, on the geometrical characteristics of the loop. The geometry considered is a set of axially symmetric corrugated pipes described by a set of parameters; namely the pipe inner radius, the period of the corrugation, the amplitude of the corrugation, and the ratio of expansion and contraction regions of a period of the pipe. The governing equations are solved using the Finite Element Method, in combination with an adaptive mesh refinement technique in order to capture the effects of wall shape. We characterize the effects of the amplitude and of the ratio of expansion and contraction. In particular we show that for a given fixed amplitude it is possible to find an optimal ratio of expansion and contraction that minimizes the temperature inside the thermosyphon. The results show that by adequately choosing the design parameters, the performance of the thermosyphon loop can be improved.

KEYWORDS: Thermosyphon, Corrugated Pipes, Shape Optimization

INTRODUCTION

Thermosyphon loops, also known as natural convection loops, are commonly employed devices in many kind of applications, ranging from solar energy utilization [1,2] to industrial applications in nuclear reactor cooling [3]. One of the main advantages of a

thermosyphon, is that the flow within the loop is driven by the buoyancy forces generated by the density gradients induced by the temperature differences in the heating and cooling sections of the loop, and therefore, it does not require a pump or another device to maintain the flow. In the cryogenic industry, thermosyphons are also commonly used, for instance, to convect a liquid from a storage vessel to a production vessel such as a pump vessel (see FIGURE 1). When such a facility is on operation, the cryogen flows out of the storage vessel towards the pump vessel, where the liquid cryogen is pumped to its final destination, a truck for instance. When the facility is not on operation, the thermosyphon return line takes the heat from the interconnecting lines to the storage vessel, thus preventing undesirable boil-off gas in the pump vessel, which would not let the pump to function properly [4]. In FIGURE 1 we have sketched the design of the thermosyphon loop, dark and light tones denote "cold" and "hot" regions respectively. The loop works as follows, cold liquid comes out of the bottom of the tank and as it flows along the pipe line towards the pump vessel, the liquid absorbs heat from the environment. The temperature differences induce buoyancy forces which drive the fluid upwards until the fluid returns to the main vessel where it cools down again.

We are concerned with the operation of such a thermosyphon loop, when the return line is composed of a so-called corrugated pipe. Corrugated pipes provide very convenient installation and maintenance possibilities in an application as an LNG delivery system. We will analyze such a system in the rest of this publication and more specifically, we will concentrate on characterizing the influence off wall-shape on the performance of the thermosyphon and we will show that the shape can be optimized for reducing the temperature inside the thermosyphon.

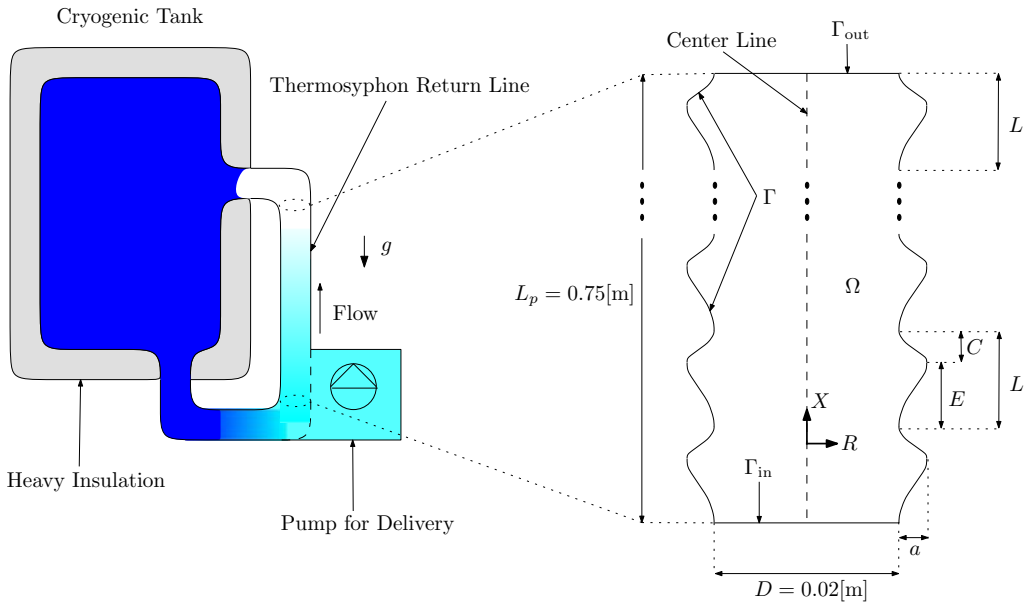

FIGURE 1. Diagram of an LNG cryogenic storage tank featuring a thermosyphon. The return line consists of a pipe (possibly corrugated) which center line is aligned with the direction of gravity.

MATERIAL PROPERTIES

Liquefied natural gas (LNG) is natural gas that has been converted temporarily to liquid form for ease of storage and transport. As a liquid, natural gas occupies only 1/600th the volume of its gaseous state, and therefore it is stored more effectively in a limited space and it is more easily transported [5]. The typical temperature at which LNG is stored is

106.95(K). Depending on the application, the storage pressure might vary from 50 (kPa), to 1700(kPa) [6]. In our case we consider LNG close to at a storage pressure of 900 (kPa). The composition of LNG is predominantly Methane, and for practical purposes, we take the properties of Methane as those of LNG. The dependency of density on temperature for Methane (CH_4) at a constant pressure of 900 (kPa), can be observed in FIGURE 2a) [7]. The density varies almost linearly for temperatures below the saturation temperature 146(K). Provided that the temperature of the LNG is below saturation, the density ρ of the LNG can be approximated by

$$\rho = \rho_0 \left[1 - \beta \left(T - T_0 \right) \right], \tag{1}$$

where ρ_0 is the density of the fluid at the reference temperature T_0, and T is the local temperature. More specifically, we have $T_0 = 106.95\,(\mathrm{K})$, $\beta = 3.7\times10^{-3}\,(\mathrm{K}^{-1})$, and $\rho_0 = 430.15\ (\mathrm{kg}\cdot\mathrm{m}^{-3})$. In FIGURE 2b), we can see how this simple linear model captures very well the variations in density. All the other properties of the fluid are taken as constant. The values which we consider are those of Methane at temperature $T_0 = 106.95\,(\mathrm{K})$, and pressure $P = 900\,(\mathrm{kPa})$. The respective values are $k = 0.1915\ \left(\mathrm{W}\cdot\mathrm{m}^{-1}\cdot\mathrm{K}^{-1}\right)$ for the thermal conductivity, $\mu = 1.3247\times10^{-4}\ \left(\mathrm{Pa}\cdot\mathrm{s}\right)$ for the dynamic viscosity, and $C = 3.4395\left(\mathrm{J}\cdot\mathrm{g}^{-1}\cdot\mathrm{K}^{-1}\right)$ for the specific heat capacity.

In addition to the properties of Methane, we need to prescribe the thermal properties of the wall. Depending on the kind of insulation, the heat transfer coefficient of transfer pipes for liquefied gases might vary from $h_1 = 0.01\ \left(\mathrm{W}\cdot\mathrm{m}^{-2}\cdot\mathrm{K}^{-1}\right)$, for heavily insulated pipes up to $h_2 = 2\ \left(\mathrm{kW}\cdot\mathrm{m}^{-2}\cdot\mathrm{K}^{-1}\right)$ for non-insulated pipes [8]. In our case, we consider two well insulated pipes, one with $h = 0.01\left(\mathrm{W}\cdot\mathrm{m}^{-2}\cdot\mathrm{K}^{-1}\right)$, and another with $h = 0.1\left(\mathrm{W}\cdot\mathrm{m}^{-2}\cdot\mathrm{K}^{-1}\right)$, the temperature of the environment is taken to be $T_0 = 290\,(\mathrm{K})$.

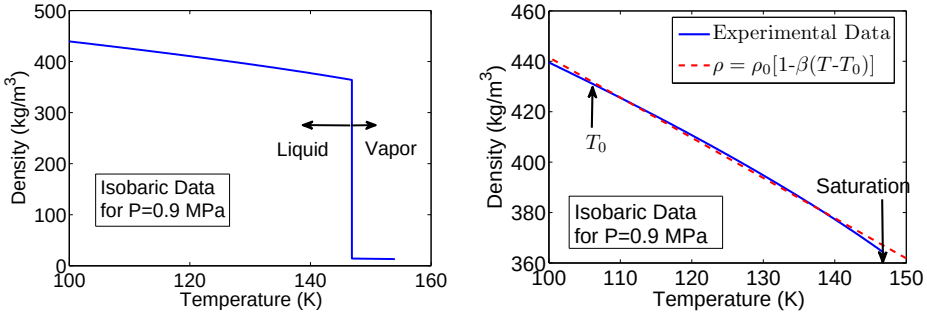

FIGURE 2. Density of Methane as function of temperature, for a constant pressure $P = 900$ (kPa). The data was taken from [7].

MODELING EQUATIONS AND GEOMETRY

The flow in a thermosyphon is driven by buoyancy forces which are a result of the density differences along the pipe. However, even though the density is not constant, the

density variations can be neglected in the momentum equation, except when they appear multiplied by the gravitational acceleration g. In other words, the flow is regarded as incompressible with respect to a reference density ρ_0, and the buoyancy effects are taken into account via a volume force term, which is directed in the opposite direction of the gravitational force g. The equations describing such a fluid are know as the Bousinnesq approximation of the Navier-Stokes equations [9-10]. The incompressibility assumption applies because the high storage pressure allows the temperature to be well bellow saturation. Since the cryogenic storage tank has very heavy insulation, most of the motion takes place along the thermosyphon return line. This line consists of two bends and a vertical section. The bends are much shorter than the vertical section, and therefore, we simply model the vertical section of the thermosyphon, denoted by Ω in FIGURE 1. The geometry is axially symmetric and periodic, with period L. Each period consists of two sections, an expansion region of length E, and a contraction region of length C. The shape of the expansion region is half a period of a sinusoidal shape with period $2E$ and amplitude a. The contraction region is half a period of a sinusoidal shape with period $2C$ and amplitude a. D denotes the inner diameter of the corrugated pipe and L_p the total length of the pipe. In the rest of this paper, we consider a geometry with $D = 0.02\,(\mathrm{m})$, $L = 5\,(\mathrm{mm})$, and $L_p = 0.75\,(\mathrm{m})$. We also define the dimensionless parameter $L_e := E/L$, which measures the proportion of expansion. Our main goal is to characterize the effects on the flow, of the amplitude a, and of the proportion of expansion L_e. In addition, we want to determine whether it is possible to find an optimal value for these parameters.

Since the geometry is axially symmetric and the center-line is aligned with the direction of gravity (see FIGURE 1), we can assume the flow to be axially symmetric as well. Assuming that the flow is steady, the modeling equations in the domain Ω are.

$$UU_x + VU_R = \nu\left(U_{XX} + U_{RR} + \frac{1}{R}U_R\right) + g\beta\left(T - T_0\right) - \frac{1}{\rho_0}P_X, \tag{2a}$$

$$UV_x + VV_R = \nu\left(V_{XX} + V_{RR} + \frac{1}{R}V_R - \frac{1}{R^2}V\right) - \frac{1}{\rho_0}P_R, \tag{2b}$$

$$U_x + V_R + \frac{1}{R}V = 0, \tag{2c}$$

$$\rho_0 C_P\left(UT_X + VT_R\right) = k\left(T_{RR} + \frac{1}{R}T_R + T_{XX}\right), \tag{2d}$$

where the corresponding variables are the axial coordinate X, the radial coordinate R, the axial velocity U, the radial velocity V, the pressure P, and the temperature T. The pressure P in the equations is the deviation from the hydrostatic pressure of a fluid with density ρ_0. The constant $\nu = \mu/\rho_0$ is the kinematic viscosity of Methane and $g = 9.806\,(\mathrm{m}\cdot\mathrm{s}^{-2})$ is the acceleration of gravity. The boundary conditions which we consider are the following.

1. The distribution of the flow and temperature are axially symmetric.

$$V = 0,\ U_R = 0,\ T_R = 0 \text{ at } R = 0. \tag{3}$$

2. The inflow and outflow are normal at the inlet Γ_{in} and at the outlet Γ_{out}. In addition, since the system forms a closed loop, the pressure change around the

loop adds up to zero. Since we already subtracted the hydrostatic pressure field within the tank, we have

$$U_X,\ P=0,\ \text{at}\ \Gamma_{\text{in}}\ \text{and}\ \Gamma_{\text{out}}. \tag{4}$$

3. The temperature at the inlet is uniform and equal to the temperature inside the tank, and at the exit, the heat is carried out mostly due to convection.

$$T_X=0\ \text{at}\ \Gamma_{\text{out}}. \tag{5}$$

4. At the wall of the pipe, a no-slip condition holds for the velocity field, and the normal heat flux is proportional to the difference of the ambient temperature and the local temperature of the fluid.

$$U=0,\ \text{V=0},\ \mathrm{n}\cdot\nabla(-kT)=h(T_e-T),\ \text{at}\ \Gamma, \tag{6}$$

here n denotes the outer unitary normal vector to the surface Γ.

NUMERICAL METHODOLOGY

The equations introduced in the previous section are solved with a mixed finite element model, with Lagrange P_2-P_1 elements for the Navier-Stokes equations, and Lagrange P_2 elements for the temperature. The order of approximation of the pressure is chosen to be one order less than the velocity, in order to avoid an overdetermined discrete system of equations [11]. The discrete nonlinear system of equations is solved using Newton iteration. The implementation was done using the code COMSOL Multyphysics [12]. After solving numerically the discrete equations, we compute the volumetric flow rate Q, the maximum temperature attained inside the thermosyphon $T_{\max}$, the average velocity $\bar{U}$, and the Reynolds number Re according to

$$Q=\int_{\Gamma_{\text{in}}} U dA,\quad T_{\max}=\max_{X\in\Omega} T(X),\quad \bar{U}=\frac{4Q}{\pi D^2},\quad \mathrm{Re}=\frac{\rho_0 \bar{U} D}{\mu}. \tag{7}$$

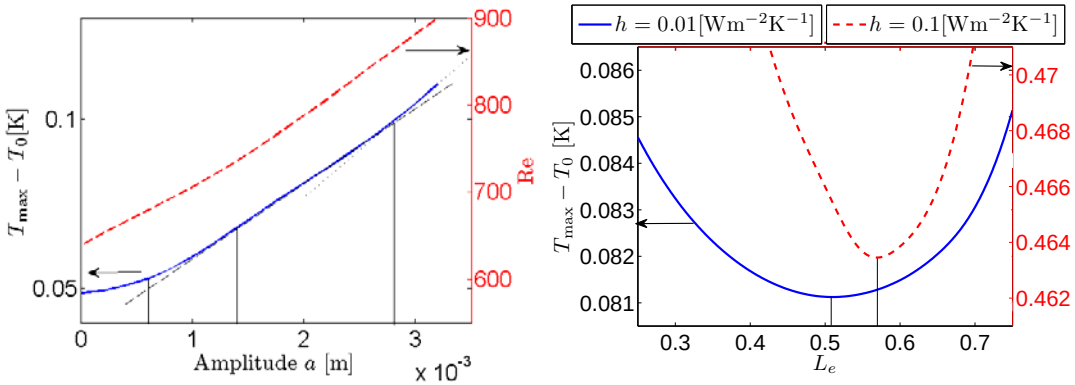

a) b)

FIGURE 3. a) Maximum increment in temperature and Reynolds number as function of the amplitude, for a heat transfer $h=0.1\ (\mathrm{W\cdot m^{-2}\cdot K^{-1}})$ b) Maximum increment in temperature as function of the parameter L_e.

The maximum temperature ($T_{\max}$) should be kept below saturation, in order to keep the liquid phase throughout the pipeline and prevent malfunctioning [13]. In order to guaranty grid independent solutions for each of the geometries considered here, we implemented a

routine which recursively refined the mesh, until the relative change in the computed volumetric flow rate Q was less than 0.1%. The adaptive refinement technique allows us to capture the effect of wall-shape on the flow. A solution with an error smaller than 0.1% was typically obtained for a mesh with 4×10^4 mesh points.

RESULTS AND DISCUSSION

We start by studying the effects of the amplitude a on the flow. In FIGURE 3a), we have plotted the maximum increase in temperature $T_{\max}-T_0$ and the Reynolds number for a geometry as in FIGURE 1, with $L=5\,(\text{mm})$, $L_e=0.5$, and wall heat transfer $h=0.1\,(\text{W}\cdot\text{m}^{-2}\cdot\text{K}^{-1})$, and various values for the amplitude a. When. $a=0\,(\text{m})$, the increment in temperature is about $T_{\max}-T_0\approx0.049\,(\text{K})$ and the Reynolds number $\text{Re}\approx638$. When we increase the amplitude of the corrugation, we obtain an increase in temperature and in the Reynolds number. For instance, when $a=2.8\,(\text{mm})$ the Reynolds number reaches a value of $\text{Re}\approx862$, and the increase in temperature is $T_{\max}-T_0\approx0.1($ K). From FIGURE 3a), we can also notice that while the Reynolds number increases almost linearly, while the temperature does not. In fact, the slope of the temperature curve increases continuously with a for values below $a\le0.6\,(\text{mm})$. Then the slope stabilizes and the temperature starts to grow almost in a linear manner around $a\approx1.4\,(\text{mm})$. As we go further, we can still appreciate a change in the slope of the curve at $a=2.8\,(\text{mm})$. To show this more clearly, we have added auxiliary dotted and dashed lines for reference.

This behavior of the increase in temperature can be explained by looking at the flow streamlines. For instance, when $a=0.6\,(\text{mm})$ (see FIGURE 4 a)) the flow follows the wall and the increase in temperature is just caused by the increase in the surface area (and therefore, also the heat transfer) with the parameter a. When we reach $a=1\,(\text{mm})$ the curve shows a linear behavior, this is associated with the appearance of a vortex inside the corrugations. For instance, when $a=1.4\,(\text{mm})$, we can observe a vortex inside the corrugations, FIGURE 4 b). The temperature continues to increase linearly, until at $a\approx2.7\,(\text{mm})$ we can observe another change in the slope of the curve. This change takes place due to the appearance of a second vortex inside the corrugation. In FIGURE 4 c), where for $a=2.8\,(\text{mm})$ we can distinguish the second vortex inside the corrugation.

In practical terms, this means that there is no amplitude which minimizes the temperature inside the thermosyphon. However, in order to have a flexible pipe line, it is necessary to have a minimum amplitude size for the corrugation. Therefore in practice, one should balance the increase in temperature and the desired flexibility of the pipe line in order to choose an optimal design value for the amplitude a.

Luckily, there is another possibility to reduce the temperature inside the thermosyphon without having to compromise the flexibility of the line. The alternative which we consider is to modify the lengths of expansion and contraction of the pipe via the parameter L_e. In Figure FIGURE 5 a) and b), we have plotted the distribution of $T_{\max}-T_0$ near the corrugations for $L_e=0.55$ and $L_e=0.7$, respectively. The wall heat transfer coefficient was $h=0.1\,(\text{W}\cdot\text{m}^{-2}\cdot\text{K}^{-1})$. When $L_e=0.7$, the heat transfer due to convection is reduced by the sharp contraction region, and this causes the temperature to raise by up to 0.47 (K). On the other hand, when $L_e=0.55$, the flow inside the cavity is able to exchange heat with the main cold stream in a more efficient way thereby reducing the maximum increase in temperature.

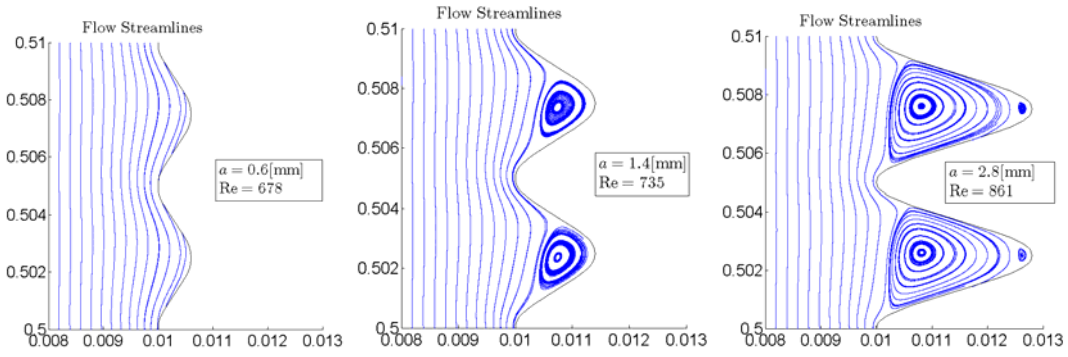

a) b) c)

FIGURE 4. Flow streamlines for three different amplitudes, for a heat transfer coefficient of $h = 0.1\,(\mathrm{W}\cdot\mathrm{m}^{-2}\cdot\mathrm{K}^{-1})$

The role of the parameter L_e becomes clearer when looking at FIGURE 3 b). In this figure we have plotted the maximum increment in temperature, $T_{\max} - T_0$, for a set of corrugated pipes with period $L = 5\,(\mathrm{mm})$ and amplitude $a = 2\,(\mathrm{mm})$, and values of L_e between 0.25 and 0.75. The solid line and left hand *y*-axis show the case for $h = 0.01\,(\mathrm{W}\cdot\mathrm{m}^{-2}\mathrm{K}^{-1})$, and the dashed line and right hand *y*-axis correspond to the case $h = 0.1(\mathrm{W}\cdot\mathrm{m}^{-2}\mathrm{K}^{-1})$. Already when $h = 0.01\,(\mathrm{W}\cdot\mathrm{m}^{-2}\mathrm{K}^{-1})$, it is possible to notice some asymmetry in the curve, even the minimum increment in temperature appears to be attained for an asymmetric geometry, i.e. for $L_e > 0.5$. When we increase the heat transfer coefficient to $h = 0.1\,(\mathrm{W}\cdot\mathrm{m}^{-2}\cdot\mathrm{K}^{-1})$, the increment in temperature $T_{\max} - T_0$, becomes more sensitive to L_e, and there is a value of L_e, of about $L_e \approx 0.57$, that minimizes the increase in temperature $T_{\max} - T_0$. Therefore, it is possible to reduce the temperature inside the thermosyphon without having to reduce the flexibility of the pipe line.

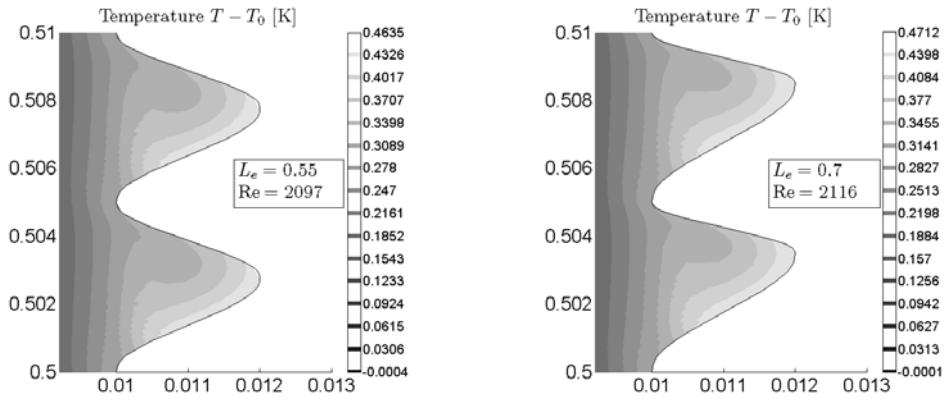

a) b)

FIGURE 5. Increase in temperature for two different values of L_e, for a wall heat transfer coefficient of $h = 0.1\,(\mathrm{W}\cdot\mathrm{m}^{-2}\cdot\mathrm{K}^{-1})$.

CONCLUSIONS

In the present paper we have presented a model for a single phase thermosyphon loop featuring corrugated pipes. By means of using an adaptive meshing technique we were able to capture the effects of wall-shape. We considered a set of asymmetric sinusoidal pipes and showed that an increase in the amplitude implies an increase in flow rate and in temperature. The appearance of vortices inside the corrugation, induce a change in the slope of the temperature as function of the amplitude a. In practical terms, this means that one should take into account this extra increment in temperature when considering changing a straight thermosyphon line by a corrugated one. In addition, we showed that when we keep the amplitude of the pipe fixed, it is possible to reduce the maximum temperature inside the thermosyphon by tuning the lengths of expansion and contraction. In fact, we showed that there is an optimal value for the parameter L_e which minimizes the increase in temperature without having to reduce the amplitude of the corrugation. The importance of the design parameter L_e is expected to increase for larger heat transfer coefficients at the wall as well as with the period of the corrugation L. Altogether, shape optimization it is very promising for improving the performance of thermosyphon. The possibility of doing shape optimization for turbulent flow is currently under research.

ACKNOWLEDGEMENTS

This work is part of a project in collaboration with Imtech SMS and it is funded by Ballast Nedam IPM.

REFERENCES

1. Siddiqui, M., *Energy Convers Manage* 38, 799–812 (1997).
2. Mertol, A., Place, W. T., and Greif, R., *Solar Energy* 27, 367–386 (1981).
3. Zvirin, Y., *Nucl. Eng. Des.* 67, 203–225 (1981).
4. Remie, P. A., and Dam, J. A. M., System and method for the delivery of LNG, Patent: World Intellectual Property Organization WO 2010/151118 A1, Ballast Nedam International Product Management B.V. (2010).
5. Parfomak, P. W., and Flynn, A. M., Liquefied Natural Gas (LNG) Import Terminals: Siting, safety and Regulation, Report for u.s. congress, CRS (2004).
6. Hightower, M. e. a., Guidance on Risk Analysis and Safety Implications of a Large Liquefied Natural Gas (LNG) Spill over Water, Tech. Rep. SAND2004-6258, Sandia National Laboratories, Albuquerque, California (2004), see also URL http://www.abc.edu.
7. Lemmon, E., McLinden, M. O., and Friend, D., editors, *Thermophysical Properties of Fluid Systems*, NIST Chemistry WebBook, NIST Standard Reference Database Number 69, National Institute of Standards and Technology, Gaithersburg MD, 20899, 2011, p.j. linstrom and w.g. mallard edn., http://webbook.nist.gov, (retrieved April 18, 2011).
8. N. GmbH, CRYOFLEX transfer lines for liquid gases, On the WWW (2010), uRL http://www.nexans.de.
9. Kundu, P. K., and Cohen, I. M., *Fluid Mechanics, Third Edition*, Elsevier Academic Press, 2004
10. Bird, R. B., and Stewart, W. E., *Transport Phenomena*, John Wiley & Sons, 2002.
11. Reddy, J. N., and Gartling, D. K., *The Finite Element Method in Heat Transfer and Fluid Dynamics*, CRC Press, 2001.
12. COMSOL, *User's Guide. COMSOL AB.* (2006).
13. Probert, S. D., Yeung, C. M., and Chu, C. Y., *Applied Energy* 12, 1–20 (1982).

PREVIOUS PUBLICATIONS IN THIS SERIES:

Number	Author(s)	Title	Month
II-40	V. Chalupecký A. Muntean	Semi-discrete finite difference multiscale scheme for a concrete corrosion model: approximation estimates and convergence	June 'II
II-41	E.H. van Brummelen K.G. van der Zee V.V. Garg S. Prudhomme	Flux evaluation in primal and dual boundary-coupled problems	July 'II
II-42	C. Mercuri M. Squassina	Global compactness for a class of quasi-linear problems	July 'II
II-43	M.V. Shenoy R.M.M. Mattheij A.A.F. v.d. Ven E. Wolterink	A mathematical model for polymer lens shrinkage	Sept. 'II
II-44	P.I. Rosen Esquivel J.H.M. ten Thije Boonkkamp J.A.M. Dam R.M.M. Mattheij	Wall shape optimization for a thermosyphon loop featuring corrugated pipes	Sept. 'II

Ontwerp: de Tantes,
Tobias Baanders, CWI